

Article

Construction of Linear Models for the Normalized Vegetation Index (NDVI) for Coffee Crops in Peru Based on Historical Atmospheric Variables from the Climate Engine Platform

Ligia García ^{1,2,*} , Jaris Veneros ^{1,*} , Manuel Oliva-Cruz ² , Neiro Olivares ¹, Segundo G. Chavez ¹ 
and Nilton B. Rojas-Briceño ³ 

¹ Instituto de Investigación para el Desarrollo Sustentable de Ceja de Selva (INDES-CES), Universidad Nacional Toribio Rodríguez de Mendoza de Amazonas, 342 Higos Urco, Chachapoyas 01001, Peru; 7180673651@untrm.edu.pe (N.O.); segundo.quintana@untrm.edu.pe (S.G.C.)

² Facultad de Ingeniería Zootecnista, Agronegocios y Biotecnología, Universidad Nacional Toribio Rodríguez de Mendoza de Amazonas, 342 Higos Urco, Chachapoyas 01001, Peru; manuel.oliva@untrm.edu.pe

³ Grupo de Investigación en Ciencia de la Información Geoespacial, Escuela Profesional de Ingeniería Ambiental, Facultad de Ingeniería y Arquitectura, Universidad Nacional de Moquegua, Pacocha 18610, Peru; nrojasb@unam.edu.pe

* Correspondence: ligia.garcia@untrm.edu.pe (L.G.); jaris.veneros@untrm.edu.pe (J.V.)

Abstract: The rapid development of digital tools for crop management offers new opportunities to mitigate the effects of climate change on agriculture. This study examines the Normalized Difference Vegetation Index (NDVI) in coffee-growing areas of the province of Rodríguez de Mendoza, southern Peru, from 2001 to 2022. The objectives were the following: (a) to analyze NDVI trends in these areas; (b) to investigate trends in climatic variables and their correlations with altitude and NDVI; and (c) to develop linear models tailored to each coffee-growing area. The study identified significant differences in NDVI trends among coffee plants, with mean NDVI values ranging from about 0.6 to 0.8. These values suggest the presence of stress conditions that should be monitored to improve crop quality, particularly in Huambo. Variability in rainfall, maximum and minimum temperatures, relative humidity, and altitude was also observed, with NDVI values showing a strong negative correlation with altitude. These results are crucial for making informed strategic decisions in integrated crop management and for monitoring crop health using vegetation indices.

Keywords: NDVI; coffee; Climate Engine; linear regression model; Rodríguez de Mendoza



Citation: García, L.; Veneros, J.; Oliva-Cruz, M.; Olivares, N.; Chavez, S.G.; Rojas-Briceño, N.B. Construction of Linear Models for the Normalized Vegetation Index (NDVI) for Coffee Crops in Peru Based on Historical Atmospheric Variables from the Climate Engine Platform. *Atmosphere* **2024**, *15*, 923. <https://doi.org/10.3390/atmos15080923>

Academic Editor: Gianni Bellocchi

Received: 15 June 2024

Revised: 24 July 2024

Accepted: 24 July 2024

Published: 1 August 2024



Copyright: © 2024 by the authors. Licensee MDPI, Basel, Switzerland. This article is an open access article distributed under the terms and conditions of the Creative Commons Attribution (CC BY) license (<https://creativecommons.org/licenses/by/4.0/>).

1. Introduction

Coffee (*Coffea arabica*) is one of the most important commodities traded worldwide [1], consumed by communities around the world. The estimate for the 2022/2023 global crop is 78.5 million bags with an increase of 1.7% [2]. In many underdeveloped countries, its cultivation, processing, and marketing support millions of jobs. In recent years, Peru has strengthened exports by cultivating approximately 425,416 ha, which has benefited the economy of 223,482 families [3], 91% of which are concentrated in seven regions: Junín, San Martín, Cajamarca, Cusco, Amazonas, Huánuco, and Pasco [4]. The Amazon region ranks 17th and 18th in terms of cultivated areas, with the districts of Omia and Lonya Grande being the most important, with 5668.46 ha and 5457.22 ha, respectively, representing 2.6% of the national cultivated area [5].

In recent times, there have been notable changes in vegetation cover and types due to global climate change and human impact. In particular, coffee cultivation has been negatively affected by extreme climatic phenomena, attributing a high vulnerability to its species [6], which is largely inferred from modeling studies based on predictions of rising temperatures and changes in precipitation patterns [7]. Thus, understanding these scenarios of vulnerability to climate change would help us preserve its biodiversity and reveal new

scenarios of choice for future breeding programs for this crop [8]. On the other hand, analyzing and understanding the atmosphere–land surface interaction is fundamental to clarifying the responses and feedback of terrestrial ecosystems to climate change [9].

The traditional method of visiting the field and surveying farmers to estimate crop yields or acquire agrometeorological data has been considered impractical, especially in situations where fields are not easily accessible; in this context, the remote sensing technique is used to successfully overcome these obstacles [10]. In addition, remote sensing techniques make it possible to obtain accurate information on crop conditions over large areas [11], facilitating the estimation of coffee productivity [12].

The NDVI is one of the most widely used vegetation indices [13]. NDVI-based models are one of the most effective analytical techniques of remote sensing used for the assessment of future crop yields [14]. This index has used important classification methods that are widely used to detect changes in land cover and land use [15,16], vegetation dynamics, and environmental studies based on time series assumption [17,18], plant productivity response to climatic variability [19], hydrological variations [20], monitoring in the improvement of drought strategy prediction [21,22], land degradation trends [22], carbon dynamics, biomass [23,24], biodiversity, and productivity [25] droughts and vegetation cover changes [26].

To download NDVI data over a time series requires intensive computational work and to access Landsat images it is necessary to have a powerful platform where we can access a large amount of images free of charge [27]. In that sense, the Climate Engine allows researchers to have free access to develop remote sensing applications for a variety of high-impact social problems, drought, deforestation, food security, water management, climate monitoring, environmental protection [28], accurate prediction of crop diseases [29], heat, extreme winds, sub-seasonal to seasonal forecasts, wildfires, crop stress, and water surface in service of the entire community [30].

Several studies rightly reinforce the individual influences of natural factors (soil types, elevation, mean annual temperature, dryness index, cumulative temperature, relief types, radiation, global radiation, vegetation types, mean annual precipitation, slope, moisture index, slope aspect) on changes in vegetation NDVI [31–33]. In addition, temporal aggregates of NDVI, obtained from satellites, could be contaminated by cloudiness; the procedure could be biased by a single false, which shows that NDVI is sensitive to false maxima and noise correction [14]. Therefore, the NDVI time series should be smoothed before use due to the noise present in the downloadable NDVI data sets [14,34].

So, knowing the individual historical values of these individual factors that influence NDVI will allow researchers to build models to predict vegetation index values, using easily available databases, with greater data accuracy and at a low cost. In recent years, the Climate Engine platform, which uses cloud computing and visualization of climate and remote sensing data for advanced monitoring of natural resources and understanding of processes, overcoming computational barriers faced by farmers, has gained ground [35].

It is worth mentioning that, nowadays, with the advances in agriculture, remote sensing is increasingly used. For example, the study of [3] evaluated the suitability of the land for coffee production, identifying a hierarchical structure based on climatological sub-criteria in pests and diseases, to support the development of sustainable agriculture. Also, Sari [12] assessed the accuracy of the land cover classification and studied the productivity of coffee cultivation using the vegetation index.

In this sense, the construction of models that allow us to infer values based on other climatic factors is crucial. For this reason, the Linear Regression Model used for this research (LRM) is useful for predicting a quantitative response and understanding relationships among variables [36]. In addition, this method is used for least squares estimation, having different ways of displaying the result of a model [37]. That is why the objective of this research was (1) to evaluate an NDVI tendencies model as a case study for 12 pixels and trends in time series ranging from 2002–2022, as well as (2) to record values for precipitation, maximum temperature, minimum temperature, relative humidity, and altitude in the

evaluated area. In turn, (3) we aim to construct general linear models for the three coffee growing areas of the Province of Rodríguez de Mendoza to understand the influence of climatic conditions on the health and density of vegetation in coffee trees, inferred from environmental variables.

2. Materials and Methods

2.1. Study Area

Three coffee growing areas in the province of Rodríguez de Mendoza, located between 1495 and 1838 MASL (Figure 1), were taken as a case example. The working unit was in the areas of Rumiaco (4 pixels), Omia (4 pixels), and Sauce (4 pixels), and the location of 12 pixels of the study area in Rodríguez de Mendoza, Peru is shown in Figure 1. Coffee has been the main product of the economy for more than 20 years.

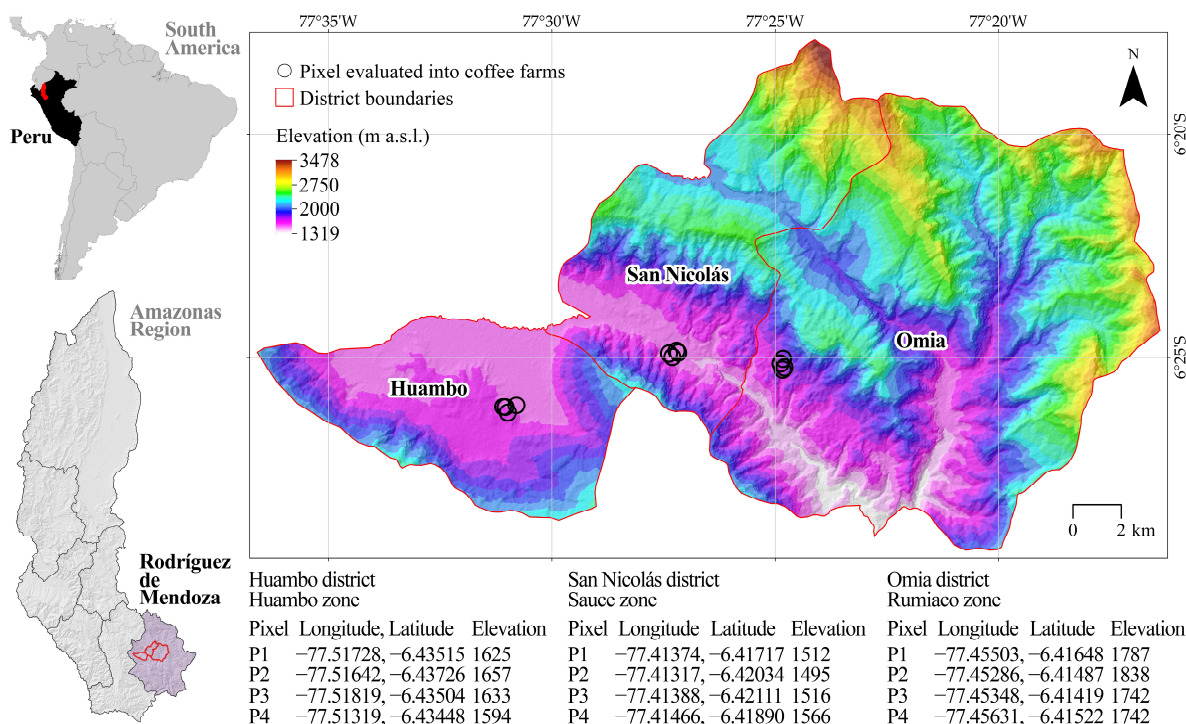


Figure 1. Geographical location of the study area in coffee crop zones of Rodríguez de Mendoza.

2.2. Historical NDVI Time Series Trends (2002–2022) in Coffee Crops

NDVI is data derived from remote sensing [38], whose formula is $R_{nir} - R_{red} / R_{nir} + R_{red}$, where there is a relationship between the difference and the sum of the red (R) and near-infrared intensities (NIR) [18] and ranges from -1 (water bodies) to 0 to 1 (vegetation) [39]. In many studies, high positive values show us that it has good photosynthetic activity, which indicates healthy vegetation [21]. Conversely, lower values that are negative close to 0 correspond to rocks, water bodies, and sand [40]. The NDVI equation correlated with photosynthetic capacity provides a tool for quantifying plant greenness and yield [41], phenology of plants [42], trophic interactions [34], plant biomass [43], and photosynthetic activity [44,45]. Also, Landsat images help to estimate NDVI with a spatial resolution of 30 m and a period of 16 days [46].

The NDVI was obtained from the open-source cloud platform Climate Engine [35,47]. We extracted the NDVI time series (Landsat 5, 7, 8, and 9 at 30 m) and climate variables from 2000 to 2022 to analyze statistical differences between pixels and between locations. Climate Engine uses the Cloud Platform, accessed and controlled through Google Earth Engine’s application programming interface (API) and its interactive development environment (IDE) to create rapid prototypes and visualize results. Most catalogs provide Landsat and Sentinel remote sensing imagery ready for analysis, at a rate of 600 scenes per day and

with a typical latency of approximately 24 h from the time of scene acquisition. From this, it provides NDVI values and climatic variables for the entire time series. These values were used to see significant differences and the construction of the linear regression model. Descriptive statistics were generated with historical NDVI data for all zones. Significant differences between pixels and between locations were calculated by the Wilcoxon test for NDVI [48] and performed in the R program 4.4.1. <https://www.r-project.org/> (accessed on 10 January 2024).

2.3. Data Acquisition for Record of Historic Trends Values for Precipitation, Temperatures Maximum, Minimum, Relative Humidity, and Correlations with Altitude and NDVI

For the historical values of the variables of precipitation (mm), maximum temperatures (°C), minimum temperatures (°C), and relative humidity (%), data download was performed from Climate Engine [49]. Then, using R studio software version 4.2.3, an analysis of historical trends (2020–2022) was made for each zone (after knowing that there are statistical differences of NVI per zone). Table 1 shows a compilation of information on the variables used in this research.

Table 1. Source and date of study variables.

Variable	Download Source	Download Date	Start and End of Download	Number of Data Downloaded (Every Factor)	Number of Data Used (Every Factor)
NDVI	http://ClimateEngine.org (accessed on 10 January 2024).	2 April 2000	25 December 2022	R = 321 H = 562 S = 559	R = 321 H = 562 S = 459
Maximum Temperatures, Minimum Temperatures, Precipitation, and Relative Humidity	http://ClimateEngine.org (accessed on 10 January 2024).	2 April 2000	25 December 2022	R = 8401 H = 8401 S = 8401	R = 8401 H = 8401 S = 8401

R = Rumiacu; H = Huambo; S = Sauce.

Based on this trend, a Pearson correlation analysis was performed between all variables for each zone using the following formula [50]:

$$r = \frac{\sum XY - (\sum X \sum Y / N)}{\sqrt{(\sum X^2 - ((\sum X)^2 / N)) (\sum Y^2 - ((\sum Y)^2 / N))}} \tag{1}$$

where N is the total number of data series.

2.4. Linear Regression Model for Coffee Crop Zones

One of the main objectives of this research is the development of a linear regression model (LRM) in the application of R Studio for the NDVI in the 12 georeferenced pixels in the coffee zones as a function of covariates such as precipitation, maximum temperature, minimum temperatures, relative humidity, and altitude for each of the pixels (12) in a time series (2000–2022). The result of this model is a formula that can be represented as the following [51]:

$$Y = Bo + B1 + E \tag{2}$$

where Y is the dependent variable (NDVI in this case), Bo, B1.. are coefficients of the terms of Y that represent independent variables, in this case (precipitation, maximum and minimum temperatures, relative humidity, and altitude), and the term E represents the error that the model tries to minimize.

To construct a linear regression model of NDVI as a function of climatic variables, the following steps were followed: (a) Data collection: historical NDVI data were collected, as well as data on the climatic variables to be included in the model (2000–2022). These data were downloaded for the same period and in three geographic areas.

For the statistical methodology, a linear regression model (LRM) of the NDVI in each zone was constructed as a function of climatic variables such as precipitation, maximum and minimum temperatures, relative humidity, and altitude, and was then performed, where NDVI is the NDVI value to be predicted and the climatic variables are the regression coefficients that indicate how each climatic variable influences the NDV. Also, (**) represents the residual error, which is the difference between the observed NDVI value and the value predicted by the model. NDVI is a measure that is used in combination to estimate the health and density of vegetation in specific geographical areas [52]. A linear regression model allows for the investigation of how NDVI is related to other variables and predicts the value of NDVI as a function of these independent variables [53]. The methodological procedure of this research is detailed in Figure 2.

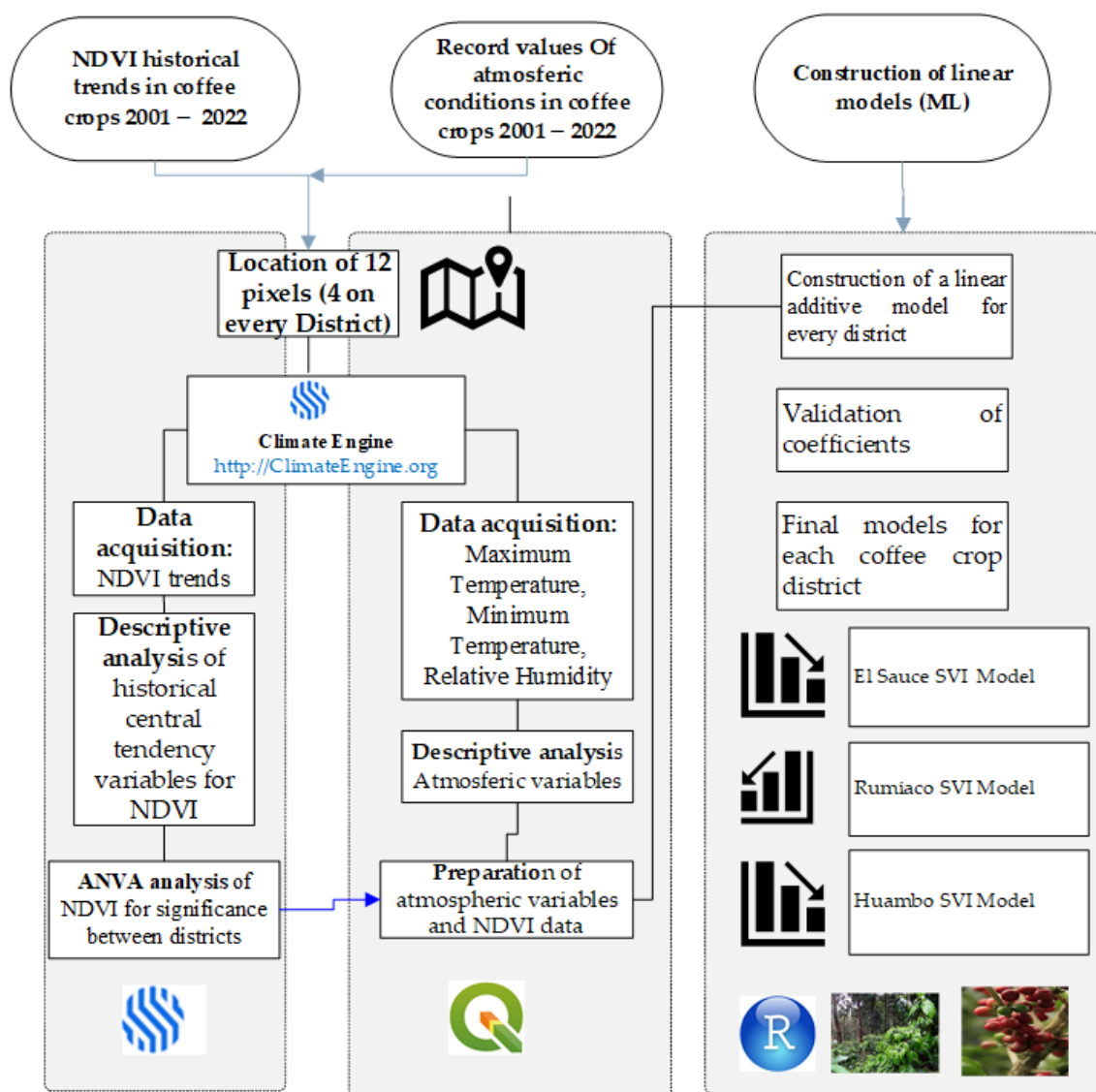


Figure 2. Conceptual methodological design.

3. Results

3.1. NDVI Historical Trends in Coffee Crop Areas (2001–2022)

Table 2 shows the true sensitivity of the 12 georeferenced pixels with coffee cultivation, showing the relationship between the standard deviation of each pixel and its mean value. Pixel N° 5 (NDVI Rumiaco) has a higher standard deviation with a value of 0.108; likewise, pixel N° 4 (NDVI Huambo) has a lower standard deviation with a value of 0.060.

Table 2. Descriptive analysis of historical central tendency variables for NDVI in 12 georeferenced points with coffee cultivation.

Pixel with Coffee Crop	Number	Mean	Standard Deviation	Standard Error	Coefficient of Variation
P1 NDVI Huambo	562	0.573 a	0.078	0.003	0.136
P2 NDVI Huambo	455	0.571 a	0.083	0.004	0.146
P3 NDVI Huambo	436	0.641 b	0.077	0.004	0.121
P4 NDVI Huambo	317	0.617 b	0.060	0.003	0.097
P9 NDVI Sauce	459	0.687 c	0.098	0.005	0.143
P12 NDVI Sauce	253	0.695 c	0.093	0.006	0.133
P7 NDVI Rumiaco	197	0.720 d	0.095	0.007	0.132
P5 NDVI Rumiaco	321	0.759 e	0.108	0.006	0.143
P6 NDVI Rumiaco	265	0.772 e	0.103	0.006	0.134
P10 NDVI Sauce	378	0.771 e	0.085	0.004	0.110
P11 NDVI Sauce	317	0.760 e	0.084	0.005	0.110
P8 NDVI Rumiaco	140	0.799 f	0.104	0.009	0.130

a, b, c, d, e, f = Tukey test for NDVI in coffee crop according to pixels. p value < 0.05 LSD = 0.02371. Error: 0.0078 df: 4088.

The Tukey test for NDVI in pixels with coffee cultivation is shown in Table 2. In this sense, six different groups are observed, where it was estimated that the highest mean value corresponds to pixel 8 with 0.80 and the lowest value corresponds to pixels 1 and 2 with 0.57 for the mean value of the index. The average values of NDVI according to pixels range from 0.573 (Huambo) to 0.799 (Rumiaco), if values closer to 1 would have greater plant greenness and greater possibilities of adaptation to changes in climatic variability.

The results of the analysis of variance for NDVI in coffee cultivation according to pixels are shown in Table 3, showing significant statistical differences between them, with a p -value of $p < 0.0001$.

Table 3. Analysis of variance for NDVI in coffee crop according to pixels.

Source of Variance	Sum of Squares	Degree of Freedom	Mean Sum of Square	F-Calc	p -Value
Model	25.63	11	2.33	300.05	<0.0001
PIXEL	25.63	11	2.33	300.05	<0.0001
Error	31.75	4088	0.01		
Total	57.38	4099			

Table 4 shows the analysis of variance indicating that there are highly significant differences in the three coffee growing zones of Rodriguez de Mendoza (Huambo, Rumiaco, and Sauce); therefore, at least each zone is different. The Huambo zone has a lower NDVI standard deviation value of 0.082. Likewise, the Rumiaco zone has a higher NDVI standard deviation value of 0.106.

Table 4. Descriptive analysis of historical central tendency variables for NDVI in 3 coffee growing areas. Descriptives—NDVI.

Place	Mean	Standard Deviation	Number
Huambo	0.597 a	0.082	1770
Suace	0.727 b	0.098	1407
Rumiaco	0.760 c	0.106	923

a, b, c = Tukey test table for NDVI in coffee cultivation according to locations.

To better understand the differences between the groups, we performed Tukey’s test in Table 4. This shows the NDVI and the Tukey test $p < 0.05$ where three different groups are observed, which indicates that the highest mean value is the Rumiaco zone, with 0.76 in group 3, and the lowest value was determined to be the Huambo zone with 0.60 in the group 1.

About the analysis of variance for NDVI in coffee crops according to locations, Table 5 shows the results of the analysis of variance, showing significant statistical differences, with a p -value of $p < 0.0001$.

Table 5. Analysis of variance for NDVI in coffee crops according to location.

Source of Variance	Sum of Squares	Degree of Freedom	Mean Sum of Square	F-Calc	p -Value
Model	21.35	2	10.67	1213.93	<0.0001
Zone	21.35	2	10.67	1213.93	<0.0001
Error	36.03	4097	0.01		
Total	57.38	4099			

3.2. Record Values of Atmospheric Conditions in Coffee Crops 2001–2022, Tendencies, and Correlations

Table 6 shows the trends of the climatic variables for the maximum, minimum, and standard deviations of the climatic variables (precipitation, maximum temperature, minimum temperature, relative humidity) in the 12 pixels of the three coffee pixels in the three districts. Although we finally unified the data of Pixels 1, 2, 3, and 4 for Huambo (Figure 3), Pixels 5, 6, 7, 8 (Figure 4) for Sauce, and Pixels 9, 10, 11, and 12 in Rumiaco (Figure 5), Table 6 shows the individual information of each pixel for the development of future individual models of prediction of vegetation indices in the sites.

Table 6. Trends of the variables, precipitation, maximum and minimum temperature, and relative humidity in pixels with coffee crops in three districts of the Province of Rodriguez de Mendoza, Peru in time series (2001–2022).

Pixel Summary		Minimum Temperatures (°C)	Precipitation (mm)	Relative Humidity (%)	Maximum Temperatures (°C)
1	Number	562	562	562	562
1	Mean	10.67	0.81	75.17	22.02
1	Standard deviation	1.47	2.52	7.51	2.05
1	Coefficient of variation	13.74	310.51	3.9	9.29
1	Minimum	6.17	0.00	33.88	17.33
1	Maximum	13.49	41.7	91.81	28.72
1	Median	10.94	0.04	75.85	21.81
1	Sum of squares	65239.5	3947.86	3207600	274810.23
2	Number	455	455	455	455
2	Mean	10.71	0.86	75.06	22.09
2	Standard deviation	1.45	2.74	7.6	2.08
2	Coefficient of variation	13.52	319.73	10.13	9.41
2	Minimum	6.17	0.00	33.88	17.33
2	Maximum	13.49	41.7	91.81	28.72
2	Median	10.89	0.04	75.81	21.97
2	Sum of squares	53120.84	3749.15	2589556	223960.13

Table 6. Cont.

Pixel Summary		Minimum Temperatures (°C)	Precipitation (mm)	Relative Humidity (%)	Maximum Temperatures (°C)
3	Number	436	436	436	436
3	Mean	10.69	0.84	74.97	22.1
3	Standard deviation	1.45	2.078	7.63	0.08
3	Coefficient of variation	13.52	332.27	10.18	9.41
3	Minimum	6.17	0	33.88	17.33
3	Maximum	13.49	41.7	91.81	28.72
3	Median	10.98	0.04	75.69	21.96
3	Sum of squares	50743.99	3663.9	2475633	214778.94
4	Number	317	317	317	317
4	Mean	10.6	0.73	74.78	22.06
4	Standard deviation	1.43	2.09	7.81	2.08
4	Coefficient of variation	13.49	285	10.45	9.44
4	Minimum	6.17	0	33.88	17.4
4	Maximum	13.49	20.25	91.12	28.49
4	Median	10.86	0.04	75.81	21.88
4	Sum of squares	36291.18	1554.29	1791757	155601.54
5	Number	321	321	321	321
5	Mean	10.62	0.86	75	21.92
5	Standard deviation	1.48	2.86	7.73	2.15
5	Coefficient of variation	13.94	331.09	10.31	9.82
5	Minimum	6.17	0	34.75	16.12
5	Maximum	13.65	41.7	91.81	28.72
5	Median	10.88	0.03	75.94	21.69
5	Sum of squares	36924.38	2863.26	1824519	155667.13
6	Number	265	265	265	265
6	Mean	10.57	0.92	74.49	22.02
6	Standard deviation	1.51	3.1	7.8	2.13
6	Coefficient of variation	14.3	336.14	10.48	9.68
6	Minimum	6.17	0	34.75	16.12
6	Maximum	13.65	41.7	91.81	28.72
6	Median	10.87	0.02	75.62	21.81
6	Sum of squares	30229	2769.45	1486493	129661.57
7	Number	197	197	197	197
7	Mean	10.56	0.75	74.29	22.08
7	Standard deviation	1.49	1.89	7.56	2.15
7	Coefficient of variation	14.07	251.56	10.18	9.73
7	Minimum	6.37	0	43.06	16.77
7	Maximum	13.65	12.42	90.94	28.72
7	Median	10.82	0.01	75.38	21.81
7	Sum of squares	22404.78	810.16	1098349	96906.16
8	Number	140	140	140	140
8	Mean	10.43	0.67	73.64	22.16
8	Standard deviation	1.53	1.9	7.61	2.13
8	Coefficient of variation	14.65	283.87	10.33	9.63
8	Minimum	6.37	0	43.06	17.02
8	Maximum	13.65	12.42	89.44	28.72
8	Median	10.39	0.01	74.81	21.8
8	Sum of squares	15548.72	564.11	767285.3	69360.24

Table 6. Cont.

Pixel Summary		Minimum Temperatures (°C)	Precipitation (mm)	Relative Humidity (%)	Maximum Temperatures (°C)
9	Number	459	459	459	459
9	Mean	10.65	0.8	75.13	21.99
9	Standard deviation	1.46	2.67	7.46	2.08
9	Coefficient of variation	13.67	331.4	9.92	9.47
9	Minimum	6.17	0	33.88	16.12
9	Maximum	13.65	41.7	91.81	28.72
9	Median	10.94	0.03	75.81	21.8
9	Sum of squares	53043.17	3553.84	2616608	223881.29
10	Number	378	378	378	378
10	Mean	10.65	0.77	74.93	22.04
10	Standard deviation	1.45	2.78	7.66	2.12
10	Coefficient of variation	13.59	361.23	10.22	9.6
10	Minimum	6.17	0	33.88	16.12
10	Maximum	13.65	41.7	91.81	28.72
10	Median	10.92	0.03	75.81	21.83
10	Sum of squares	43688.66	3139.46	2144594	185330.92
11	Number	317	317	317	317
11	Mean	10.58	0.8	75.06	21.99
11	Standard deviation	1.47	2.99	7.17	2.11
11	Coefficient of variation	13.91	371.9	9.55	9.59
11	Minimum	6.37	0	43.06	16.12
11	Maximum	13.65	41.7	91.81	28.72
11	Median	10.82	0.03	75.81	21.73
11	Sum of squares	36168.98	3026.33	1802337	154689.45
12	Number	253	253	253	253
12	Mean	10.62	0.82	74.92	22.08
12	Standard deviation	1.47	3.09	7.13	2.12
12	Coefficient of variation	13.85	374.81	9.51	9.61
12	Minimum	6.37	0	45.12	16.12
12	Maximum	13.65	41.7	91.81	28.72
12	Median	10.83	0.03	75.69	21.88
12	Sum of squares	29059.21	2569.99	1432929	124472.26

After correlating variables, using historical trend data for each zone (Figure 6), NDVI values were found to have a weak significant negative correlation with elevation in Huambo and Sauce. In addition, they have a weak positive correlation with the minimum temperatures in Rumiacu. Although the NVI values do not have a significant historical association with the other variables, the trends and variations in the correlations between them are changing. In the three zones, for example, maximum temperature is strongly positively correlated with minimum temperature and negatively correlated with precipitation and relative humidity; minimum temperature is strongly positively correlated with precipitation and relative humidity. It was also found that the higher the precipitation, the higher the relative humidity.

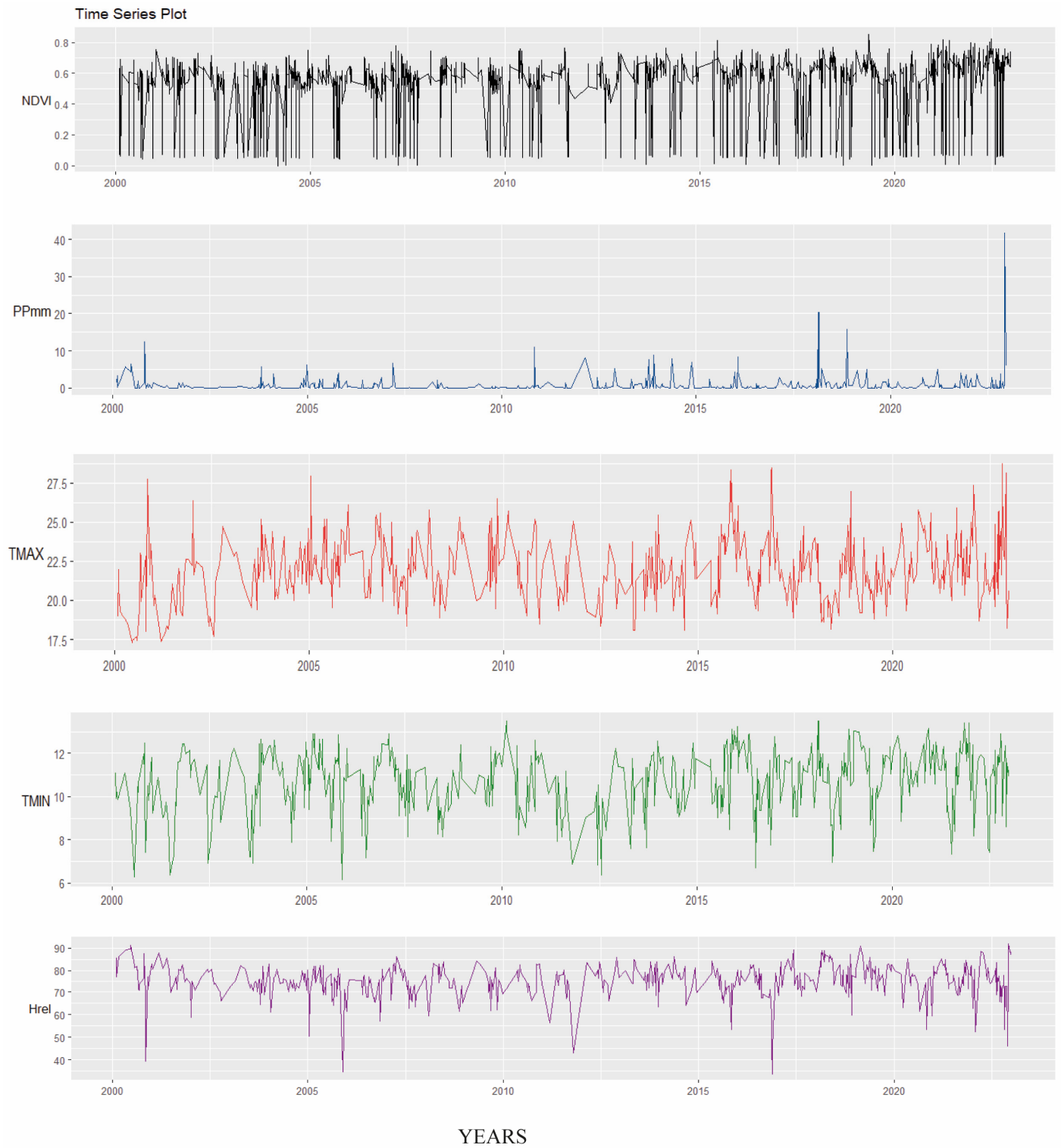


Figure 3. Time series plot for NDVI and climatic variables in Huambo.

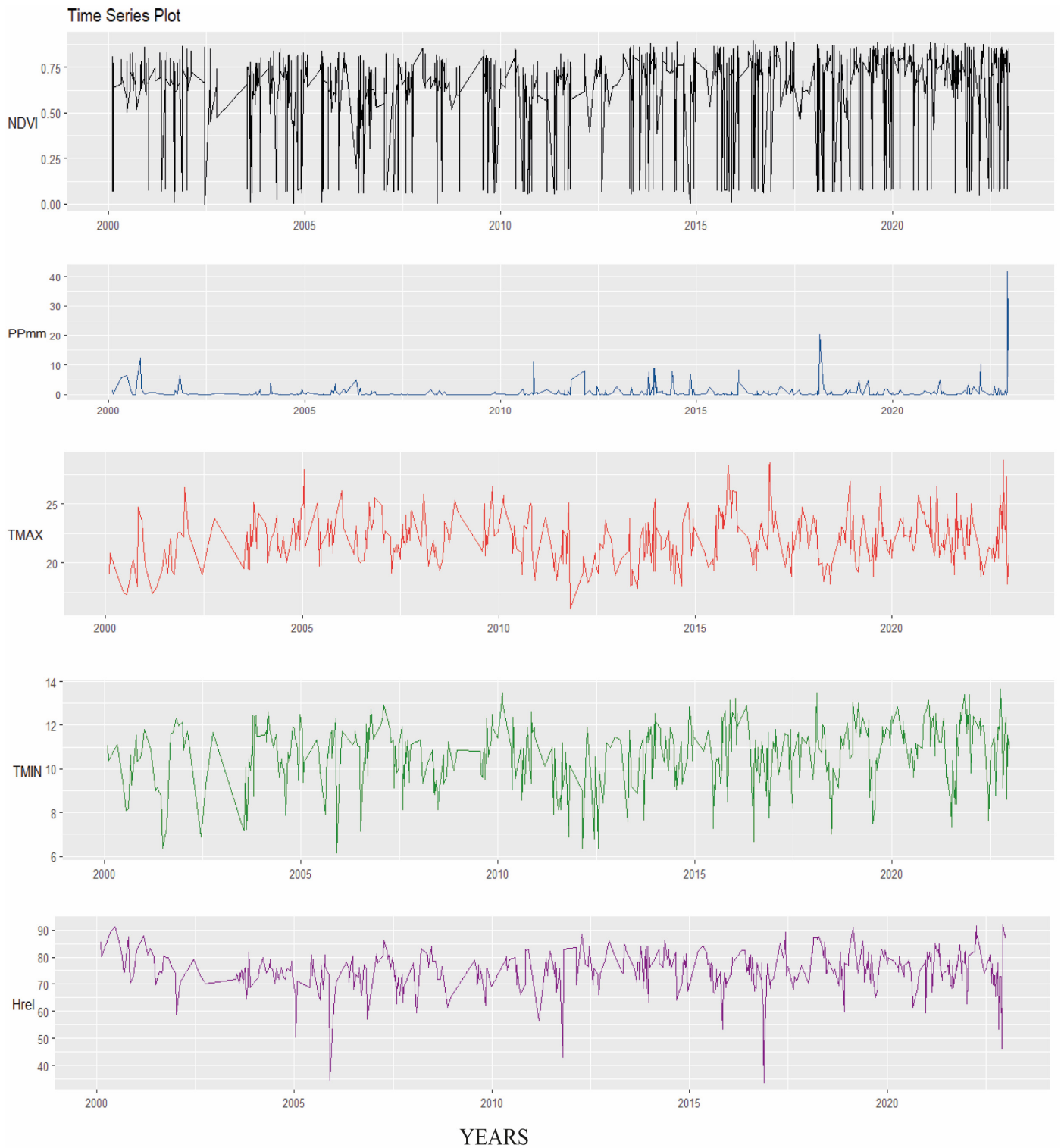


Figure 4. Time series plot for NDVI and climatic variables in Sauce.

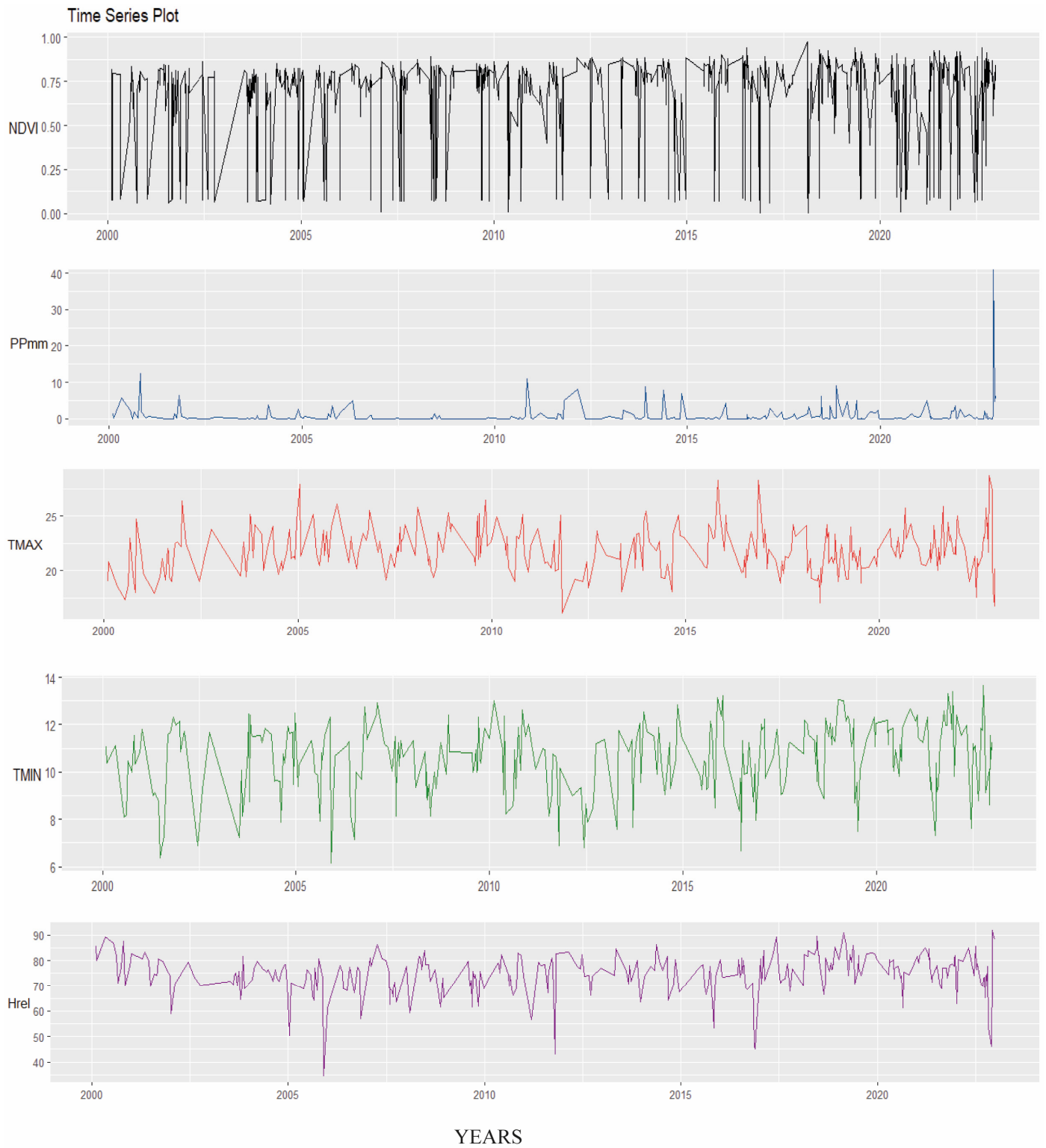


Figure 5. Time series plot for NDVI and climatic variables in Rumiacu.

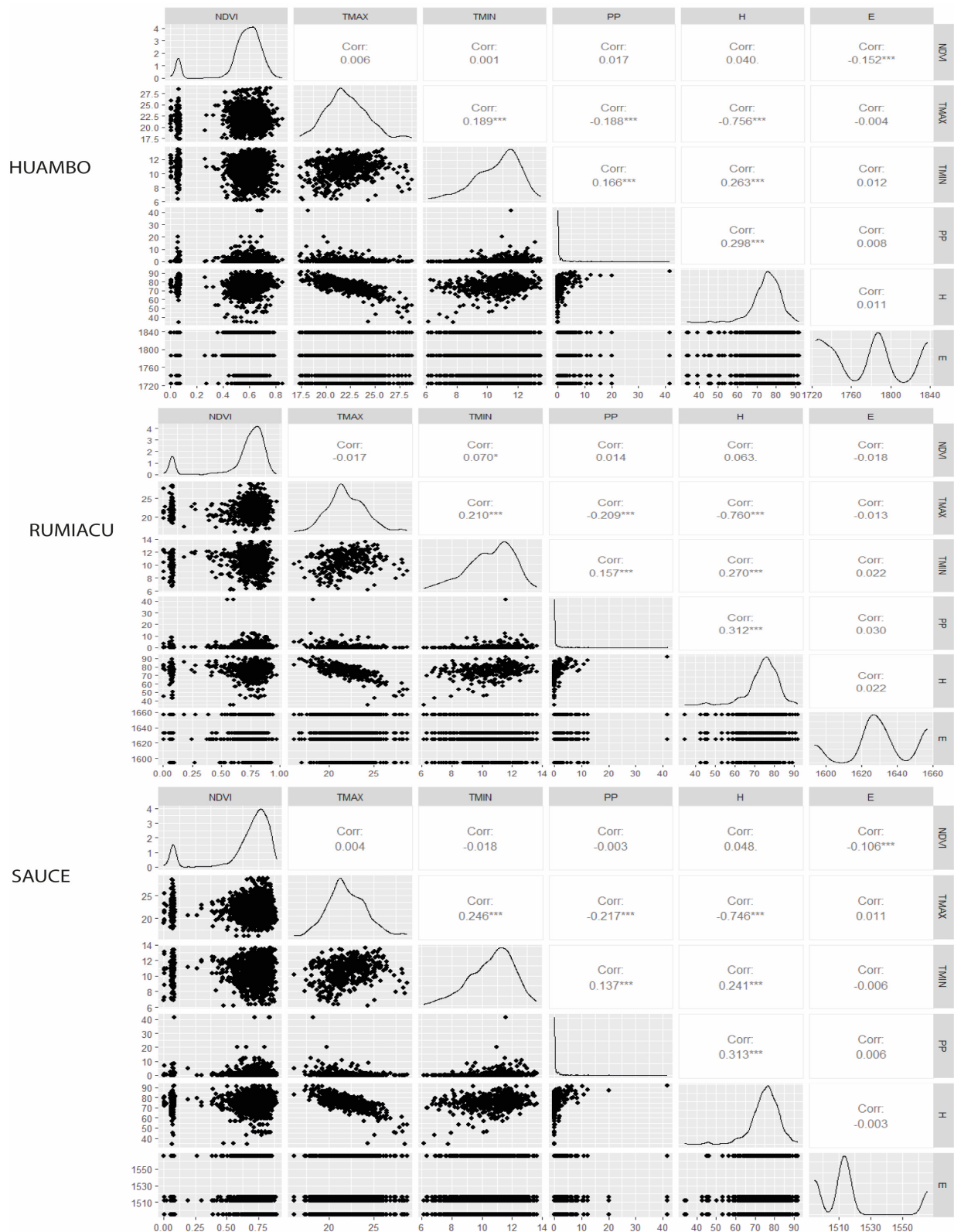


Figure 6. Plot correlation for the climatic variables, elevation, and NDVI according to the study area. * = significance $p < 0.05$; ** = significance $p < 0.01$; *** = significance $p < 0.001$.

3.3. Linear Regression Model

The linear regression model NDVI, as a function of climatic variables, such as precipitation, maximum and minimum temperature, relative humidity, and altitude, allowed us

to understand the influence of climatic conditions on the health and density of vegetation in the three study zones. In this sense, a linear regression analysis was carried out to model the NDVI as a function of the five climatic variables for the three coffee growing zones, as shown below.

3.3.1. Model for Sauce

$$1.5037778 \text{ NDVI} \sim 0.0144962 \text{ TMAX} + (-0.0103273 \text{ TMIN}) + 0.0043354 \text{ H} + (-0.0008636 \text{ ALT})$$

The coefficient of maximum temperature (0.0144962) indicates a positive relationship between maximum temperature and NDVI. As the maximum temperature increases by one degree Celsius, on average, NDVI tends to increase by 0.0144962 units. In turn, the coefficient of minimum temperature (−0.0103273) indicates a negative relationship between minimum temperature and NDVI. However, as the minimum temperature increases, the average NDVI tends to decrease.

The relative humidity coefficient (0.0043354) indicates a positive relationship between relative humidity and NDVI. As relative humidity decreases, on average, NDVI tends to increase by 0.0043354 units. On the other hand, the coefficient of altitude (- 0.0008636) indicates a negative relationship between altitude and NDVI. As altitude increases, on average, NDVI tends to decrease.

The R2 value is 0.06708, which means that 60% of the variability in NDVI can be explained by the climatic variables included in the model.

3.3.2. Model for Rumiaco

$$0.3052925 \text{ NDVI} \sim 0.0156559 \text{ TMAX} + (-0.0148322 \text{ TMIN}) + 0.0035842 \text{ H}$$

The coefficient of maximum temperature (0.0156559) indicates a positive relationship between maximum temperature and NDVI. As the maximum temperature increases by one degree Celsius, on average, NDVI tends to increase by 0.0156559 units. At the same time, the minimum temperature coefficient (−0.0148322) indicates a negative relationship between minimum temperature and NDVI. As the minimum temperature increases, on average, the NDVI tends to decrease.

The relative humidity coefficient (0.0035842) indicates a positive relationship between relative humidity and NDVI. As relative humidity decreases, on average, NDVI tends to increase by 0.0035842 units. Therefore, the R2 value is 0.026, which means that 20% of the variability in NDVI can be explained by the climatic variables included in the model.

3.3.3. Model for Huambo

$$1.0137 \text{ NDVI} \sim 1.037 \text{ TMAX} + (-5.789 \text{ TMIN}) + 4.013 \text{ H} + -6.291 \text{ ALT}$$

The coefficient of maximum temperature (1.037) indicates a positive relationship between maximum temperature and NDVI. As maximum temperature increases by one degree Celsius, on average, NDVI tends to increase by 1.037 units. In parallel, the minimum temperature coefficient (−5.789) indicates a negative relationship between minimum temperature and NDVI. As the minimum temperature increases the average NDVI tends to decrease. On the other hand, the coefficient of relative humidity (4.013) indicates a positive relationship between relative humidity and NDVI. As the percentage of relative humidity decreases, on average, NDVI tends to increase by 4.013 units. Consequently, the R2 value is 0.026, this means that 20% of the variability in NDVI can be explained by the climatic variables included in the model.

The coefficient of altitude (−6.291) indicates a negative relationship between altitude and NDVI. As altitude increases, on average, NDVI tends to decrease. Consequently, the R2 value is 0.1469, which means that 14% of the variability in NDVI can be explained by the climatic variables included in the model.

4. Discussion

4.1. NDVI Trends in Coffee Crop Areas in the Time Series Ranging from 2000–2022

The Normalized Vegetation Index (NDVI) is a satellite product that is increasingly gaining popularity in the world of agriculture [54]. The NVI is used in all types of studies in different production chains [55], such as those of Peruvian coffee through the present research. Likewise, other chains, such as rice cultivation [56], avocado and grape cultivation [57], crops such as wheat, sunflower, cotton, beans, watermelon, asparagus, watermelon, onion, basil [58], and corn [59], among other crops, especially coffee [60], as shown in this research.

In this sense, the NDVI ranges are represented from -1 to 1 [61], and for this research on coffee crops, they are represented between 0.573 (Huambo) and 0.799 (Rumiacu). Studies in avocado (*Persea americana* Mill) obtained NDVI values ranging from -0.65 to 0.26 [62], with very low NDVI values obtained in the dry season, while negative values were due to plots with dead trees. Researchers performed an empirical analysis under the NDVI curve and crop yield and obtained an average R^2 of 0.86 for corn and 0.80 for soybean [63]. Meanwhile, a study focused on fertilizer application and crop yield in rice and wheat [64] obtained NDVI values $R^2 = 0.601$ – 0.809 , which were effective in predicting yield and application. In the case of cereals, a relationship was established between grain yield and NDVI, where strong correlations were shown ranging from 0.70 to 0.89 [65]. This is essential for decision-making in food security.

Regarding NDVI values in coffee cultivation, Rivera and collaborators obtained values higher than 0.8 in coffee cultivation of the castle variety, which means that the plant has a good nutritional status in two phenological periods [66]; therefore, values lower than 0.8 in the three evaluated zones (Rumiacu, Sauce, and Huambo) could be revised under the approach of inadequate management of the nutritional status of coffee. Likewise, the evaluated NDVI in coffee growing areas obtained in one area values greater than 0.75 in coffee cultivation [67]. This represents a high vegetative vigor that can be used to define new areas with coffee plantations. Predictions were made to determine the phenological stage of the coffee crop using NDVI over a period of time [68], where it was observed that the NDVI decreases in the harvesting periods, such as period 1 (R^2 0.82 – 0.49) and period 2 (R^2 0.87 – 0.45), based on a polynomial regression. Therefore, standard deviations in the NDVI trends of up to 0.104 of the evaluated coffee plants suggest that they are related to the different phenological stages of the coffee plants at the time of the evaluation. NDVI values were also analyzed in healthy coffee plants and plants infested by leaf miner bugs (*Leucoptera coffeella*), achieving a result of an NDVI value for a healthy plant of (0.70), a value for infested plant of (0.58), and a value for plants infested in mines by leaf miners of (0.42), concluding that both have a green color, and the values exceed 0.50 [69]. These ranges of NDVI values, like this research, demonstrate the need for exhaustive analyses in the fields of Rumiacu, Sauce, and Huambo to assess the sensitivity of the index to the presence of pests and diseases such as *Leucoptera coffeella*.

4.2. Values for Atmospheric Conditions in Coffee Crops from 2001–2022: Tendencies and Correlations

As the NDVI is related to meteorological variables such as maximum and minimum temperature, precipitation, relative humidity, and altitude [70–72], the average NDVI values are between 0.573 (Huambo) and 0.799 (Rumiacu); these values, obtained in the coffee areas investigated here, have a degree of relationship with each meteorological variable, which is important to estimate. Therefore, it is essential to know the optimal ranges of these values for coffee cultivation. In this sense, rainfall is one of the main factors that affect the growth of coffee plantations, and high levels of rainfall provide better growth for the crops and vegetation [73]; consideration should be given to the significant positive relationship with maximum temperature in coffee-growing areas such as those presented in this research. However, during the last few years, there have been notorious changes in the growth of coffee crops and vegetation cover due to the increase in climatic variables,

which significantly affected the growth of coffee crops and vegetation cover due to climate change [71].

In this sense, concerning the climatic variables, statistically significant relationships were shown between the variables in the coffee growing zones, which are characterized by differences between temperatures, precipitation, relative humidity, and altitude. Precipitation (mm) is one of the meteorological parameters of the perennial coffee crop and is of major importance, which is difficult to predict, measure, and verify [74] as it is related to the phenology of coffee cultivation [75]. Therefore, the historical highest values of the maximum measurement were presented in pixels 1, 2, 3, 5, 6, 9, 10, 11, and 12 (41.70), and the lowest value of the maximum measurement was presented in pixels 7 and 8 (0.25) (21 February 2018). The values recorded in the present research represent a change in the distribution of precipitation in coffee-growing areas. It is therefore detrimental to vegetative development, showing that it is sensitive to changes in climate [76]. On the other hand, in its temporal variations of relative humidity, it was characterized by high peaks, with minimum values of 91.81% (8 December 2022) and maximums of the mean of 89.44% on 21 June 2018

Likewise, temperature is a variable that affects the vegetative growth of the coffee crop [77]. When there is an increase in minimum temperature, there may have been a development of vegetation; therefore, it is the temperature factor that inhibits the growth of vegetation in the three coffee growing zones. However, an increase in the maximum temperature may have inhibited the growth of the coffee crop and reduced the growth of vegetation, weakening photosynthesis [71]. In the case of coffee cultivation, it does not tolerate a wide range of temperatures [78]. On the other hand, researchers indicate that the optimum average temperatures for coffee crops are between 15 and 25 °C, with 10 °C of daily oscillation, and the optimum temperature range for coffee plantations is between 18 and 21 °C (64 and 70 °C) [79].

Taking advantage of the recent advances that exist, climatic variables affect the vegetative development and phenology of the coffee crop. The effect of temperature on the vegetative growth and flowering of nine coffee cultivars was investigated, and all cultivars showed rapid growth during summer and autumn [77].

4.3. Linear Model According to Locations

The performance of the LM was evaluated with different factors, including multicollinearity, predictor variables, error coefficient, and sample size [37], concluding that all model estimates generally perform differently for the three zones evaluated.

In this study, it was observed that the variables (temperature, relative humidity, and altitude) are highly significant for creating linear regression models that explain the NDVI of each study area. In this regard, researchers' studies include other variables such as specific land use and vegetation structure, as these could limit the influence of external or confounding factors on the relationship between vegetation types and NDVI [80]. It is also noted that linear models are more advantageous for predicting crop yields [81]. It was currently found that the linear mixed model can model growth curves with high accuracy for tomato plants in an open field [82]. However, for all case studies, the importance of delineating the boundary between agricultural and non-agricultural land is highlighted to have a better fit and not contaminate the NDVI–crop yield relationship [83,84].

5. Conclusions

Our analysis of the NDVI trend in coffee crops in three districts of Rodriguez de Mendoza during the period ranging from 2000 to 2022 reveals average values from 0.597 to 0.760, denoting certain stress conditions that deserve to be monitored for crop quality improvement. The absence of average NDVI values below 0.500 demonstrates that the coffee crop can still be produced under these conditions. In addition, the lower values presented in Huambo, in relation to the mean NDVI and for the standard deviation,

denote a lower photosynthetic activity that exposes the plant to conditions of greater stress, compared to Sauce and Rumiacu.

Although NDVI values only show strong negative correlations with elevation, the strong positive and negative correlations of elevation with the other climatic variables (minimum temperature, precipitation, relative humidity, maximum temperature) allowed the generation of general linear models for each study area. The general linear models are different for each study area and could be generated considering the historical trends of the climatic variables.

This research confirms the great applicability of easily accessible satellite technology tools (such as the Climate Engine platform) that allow the generation of management strategies for the environment and the improvement of coffee cultivation in the future.

Author Contributions: Conceptualization, L.G., S.G.C. and J.V.; methodology, L.G., J.V., M.O.-C., N.O. and S.G.C.; software, L.G., J.V. and N.B.R.-B.; validation, L.G., J.V. and N.B.R.-B.; formal analysis, M.O.-C., N.O. and S.G.C.; investigation, L.G., J.V. and N.B.R.-B.; resources, M.O.-C. and L.G.; data curation, S.G.C.; writing—original draft preparation, M.O.-C., N.O., S.G.C. and N.B.R.-B.; writing—review and editing, L.G. and J.V.; visualization, M.O.-C. and N.O.; supervision, L.G.; project administration, L.G.; funding acquisition, M.O.-C. All authors have read and agreed to the published version of the manuscript.

Funding: The study was funded by the Instituto de Investigación para el Desarrollo Sustentable de Ceja de Selva (INDES-CES) in the project CEINCAFE (C.U.I. N° 2317883—CEINCAFÉ), the ApiGen Project (CONTRATO N° PE501083491-2023-PROCIENCIA), and the CoffeSmart Project (CONTRATO N° PE501086357-2024-PROCIENCIA), of the Universidad Nacional Toribio Rodríguez de Mendoza de Amazonas del Perú.

Institutional Review Board Statement: Not applicable.

Informed Consent Statement: Not applicable.

Data Availability Statement: Data are contained within the article.

Acknowledgments: Thanks to the Universidad Nacional Toribio Rodríguez de Mendoza de Amazonas (UNTRM) for research support and economic funds.

Conflicts of Interest: The authors declare no conflict of interest.

References

1. Pancsira, J. International Coffee Trade: A Literature Review. *J. Agric. Inform.* **2022**, *13*, 26–35. [CrossRef]
2. International Coffee Organization. *Diversification; Promotion; and Upgrading Coffee Production and Marketing*; 23AD; International Coffee Organization: London, UK, 2023.
3. Salas López, R.; Gómez Fernández, D.; Silva López, J.O.; Rojas Briceño, N.B.; Oliva, M.; Terrones Murga, R.E.; Iliquín Trigoso, D.; Barboza Castillo, E.; Barrera Gurbillón, M.Á. Land Suitability for Coffee (*Coffea arabica*) Growing in Amazonas, Peru: Integrated Use of AHP, GIS and RS. *ISPRS Int. J. Geo-Inf.* **2020**, *9*, 673. [CrossRef]
4. Chichipe Oyarce, J.; Camacho, A.; Bobadilla, L.G.; Vigo, C.N.; Vásquez, H.V.; Silva Valqui, G. Clonal Propagation of *Coffea arabica* with Indole Butyric Acid and Acclimatization Conditions in Amazonas, Peru. *Int. J. Agron.* **2021**, *2021*, 8590590. [CrossRef]
5. Vargas, C.D.; Willems, M.C. *Línea Base del Sector Café en Perú*; Programa de las Naciones Unidas para el Desarrollo—PNUD: Lima Peru, 2017; Available online: <https://camcafeperu.com.pe/admin/recursos/publicaciones/Linea-base-del-sector-cafe-en-Peru.pdf> (accessed on 25 July 2024).
6. Tapaça, I.d.P.E.; Mavuque, L.; Corti, R.; Pedrazzani, S.; Maquia, I.S.A.; Tongai, C.; Partelli, F.L.; Ramalho, J.C.; Marques, I.; Ribeiro-Barros, A.I. Genomic Evaluation of *Coffea arabica* and Its Wild Relative *Coffea racemosa* in Mozambique: Settling Resilience Keys for the Coffee Crop in the Context of Climate Change. *Plants* **2023**, *12*, 2044. [CrossRef] [PubMed]
7. Damatta, F.M.; Avila, R.T.; Cardoso, A.A.; Martins, S.C.V.; Ramalho, J.C. Physiological and Agronomic Performance of the Coffee Crop in the Context of Climate Change and Global Warming: A Review. *J. Agric. Food Chem.* **2018**, *66*, 5264–5274. [CrossRef]
8. Chalchissa, F.B.; Diga, G.M.; Tolossa, A.R. Modeling the Responses of Coffee (*Coffea arabica* L.) Distribution to Current and Future Climate Change in Jimma Zone, Ethiopia. *Sains Tanah* **2022**, *19*, 19–32. [CrossRef]
9. Zhao, W.; Hu, Z.; Guo, Q.; Wu, G.; Chen, R.; Li, S. Contributions of Climatic Factors to Interannual Variability of the Vegetation Index in Northern China Grasslands. *J. Clim.* **2020**, *33*, 175–183. [CrossRef]
10. Shrestha, R.; Di, L.; Yu, E.G.; Kang, L.; Li, L.; Shahinoor Rahman, M.; Deng, M.; Yang, Z. Regression Based Corn Yield Assessment Using MODIS Based Daily NDVI in Iowa State. In Proceedings of the 2016 Fifth International Conference on Agro-Geoinformatics (Agro-Geoinformatics), Tianjin, China, 18–20 July 2016.

11. Atzberger, C. Advances in Remote Sensing of Agriculture: Context Description, Existing Operational Monitoring Systems and Major Information Needs. *Remote Sens.* **2013**, *5*, 949–981. [[CrossRef](#)]
12. Sari, D.N.; Sasmito, B.; Hadi, F.; Kurniawan, D.A. Estimasi Produktivitas Kopi Dengan Indeks Vegetasi Menggunakan Citra SPOT-7. *Elipsoida J. Geod. Dan Geomatika* **2022**, *5*, 44–52. [[CrossRef](#)]
13. Xu, Y.; Dai, Q.Y.; Zou, B.; Xu, M.; Feng, Y.X. Tracing Climatic and Human Disturbance in Diverse Vegetation Zones in China: Over 20 Years of NDVI Observations. *Ecol. Indic.* **2023**, *156*, 111170. [[CrossRef](#)]
14. Huang, S.; Tang, L.; Hupy, J.P.; Wang, Y.; Shao, G. A Commentary Review on the Use of Normalized Difference Vegetation Index (NDVI) in the Era of Popular Remote Sensing. *J. For. Res.* **2021**, *32*, 1–6. [[CrossRef](#)]
15. Aburas, M.M.; Abdullah, S.H.; Ramli, M.F.; Ash'aari, Z.H. Measuring Land Cover Change in Seremban, Malaysia Using NDVI Index. *Procedia Environ. Sci.* **2015**, *30*, 238–243. [[CrossRef](#)]
16. Berkessa, Y.W.; Bulto, T.W.; Moisa, M.B.; Gurmessa, M.M.; Werku, B.C.; Juta, G.Y.; Negash, D.A.; Gemedo, D.O. Impacts of Urban Land Use and Land Cover Change on Wetland Dynamics in Jimma City, Southwestern Ethiopia. *J. Water Clim. Chang.* **2023**, *14*, 2397–2415. [[CrossRef](#)]
17. Chen, J.; Jönsson, P.; Tamura, M.; Gu, Z.; Matsushita, B.; Eklundh, L. A Simple Method for Reconstructing a High-Quality NDVI Time-Series Data Set Based on the Savitzky-Golay Filter. *Remote Sens. Environ.* **2004**, *91*, 332–344. [[CrossRef](#)]
18. Dagnachew, M.; Dagnachew, M.; Kebede, A.; Moges, A.; Abebe, A. Effects of Climate Variability on Normalized Difference Vegetation Index (NDVI) in the Gojeb River Catchment, Omo-Gibe Basin, Ethiopia. *Adv. Meteorol.* **2020**, *2020*, 8263246. [[CrossRef](#)]
19. Crichton, K.A.; Anderson, K.; Charman, D.J.; Gallego-Sala, A. Seasonal Climate Drivers of Peak NDVI in a Series of Arctic Peatlands. *Sci. Total Environ.* **2022**, *838*, 156419. [[CrossRef](#)] [[PubMed](#)]
20. Jiang, F.; Kuang, R.; Xia, A.; Feng, Q.; Zhou, M. Variation Characteristics of Poyang Lake Water Area and Its Response to Meteorological Factors in the Past 35 Years. *J. Water Clim. Chang.* **2023**, *14*, 2706–2718. [[CrossRef](#)]
21. Gelata, F.T.; Jiqin, H.; Gemedo, S.C.; Asefa, B.W. Application of GIS Using NDVI and LST Estimation to Measure Climate Variability-Induced Drought Risk Assessment in Ethiopia. *J. Water Clim. Chang.* **2023**, *14*, 2479–2489. [[CrossRef](#)]
22. Wei, H.; Liu, X.; Hua, W.; Zhang, W.; Ji, C.; Han, S. Copula-Based Joint Drought Index Using Precipitation, NDVI, and Runoff and Its Application in the Yangtze River Basin, China. *Remote Sens.* **2023**, *15*, 4484. [[CrossRef](#)]
23. Anand, A.; Pandey, P.C.; Petropoulos, G.P.; Pavlides, A.; Srivastava, P.K.; Sharma, J.K.; Malhi, R.K.M. Use of Hyperion for Mangrove Forest Carbon Stock Assessment in Bhitarkanika Forest Reserve: A Contribution towards Blue Carbon Initiative. *Remote Sens.* **2020**, *12*, 597. [[CrossRef](#)]
24. Baniya, B.; Tang, Q.; Huang, Z.; Sun, S.; Techato, K. anan Spatial and Temporal Variation of NDVI in Response to Climate Change and the Implication for Carbon Dynamics in Nepal. *Forests* **2018**, *9*, 329. [[CrossRef](#)]
25. Wang, R.; Gamon, J.A.; Montgomery, R.A.; Townsend, P.A.; Zygielbaum, A.I.; Bitan, K.; Tilman, D.; Cavender-Bares, J. Seasonal Variation in the NDVI-Species Richness Relationship in a Prairie Grassland Experiment (Cedar Creek). *Remote Sens.* **2016**, *8*, 128. [[CrossRef](#)]
26. Veneros, J.E.; García, L. Application of the Standardized Vegetation Index (SVI) and Google Earth Engine (GEE) for Drought Management in Peru. *Trop. Subtrop. Agroecosyst.* **2022**, *25*, 1–13. [[CrossRef](#)]
27. Liao, L.; Song, J.; Wang, J.; Xiao, Z.; Wang, J. Bayesian Method for Building Frequent Landsat-like NDVI Datasets by Integrating MODIS and Landsat NDVI. *Remote Sens.* **2016**, *8*, 452. [[CrossRef](#)]
28. Gorelick, N.; Hancher, M.; Dixon, M.; Ilyushchenko, S.; Thau, D.; Moore, R. Google Earth Engine: Planetary-Scale Geospatial Analysis for Everyone. *Remote Sens. Environ.* **2017**, *202*, 18–27. [[CrossRef](#)]
29. Ibrahim, E.S. Predicting Potato Diseases in Smallholder Agricultural Areas of Nigeria Using Machine Learning and Remote Sensing-Based Climate Data. *PhytoFrontiers* **2024**, *4*, 89–105. [[CrossRef](#)]
30. Degano, M.F.; Rivas, R.E. Evaluación de Los Productos de Evapotranspiración Disponibles En Climate Engine y Del Algoritmo Support Vector Machine Regression Con Datos NASA Power. *Rev. Geol. Apl. Ing. Ambiente* **2023**, *50*, e005.s. [[CrossRef](#)]
31. Peng, W.; Kuang, T.; Tao, S. Quantifying Influences of Natural Factors on Vegetation NDVI Changes Based on Geographical Detector in Sichuan, Western China. *J. Clean. Prod.* **2019**, *233*, 353–367. [[CrossRef](#)]
32. Lamchin, M.; Lee, W.K.; Jeon, S.W.; Wang, S.W.; Lim, C.H.; Song, C.; Sung, M. Long-Term Trend and Correlation between Vegetation Greenness and Climate Variables in Asia Based on Satellite Data. *Sci. Total Environ.* **2018**, *618*, 1089–1095. [[CrossRef](#)] [[PubMed](#)]
33. Qu, S.; Wang, L.; Lin, A.; Zhu, H.; Yuan, M. What Drives the Vegetation Restoration in Yangtze River Basin, China: Climate Change or Anthropogenic Factors? *Ecol. Indic.* **2018**, *90*, 438–450. [[CrossRef](#)]
34. Pettorelli, N.; Vik, J.O.; Mysterud, A.; Gaillard, J.M.; Tucker, C.J.; Stenseth, N.C. Using the Satellite-Derived NDVI to Assess Ecological Responses to Environmental Change. *Trends Ecol. Evol.* **2005**, *20*, 503–510. [[CrossRef](#)] [[PubMed](#)]
35. Huntington, J.L.; Hegewisch, K.C.; Daudert, B.; Morton, C.G.; Abatzoglou, J.T.; McEvoy, D.J.; Erickson, T. Climate Engine: Cloud Computing and Visualization of Climate and Remote Sensing Data for Advanced Natural Resource Monitoring and Process Understanding. *Bull. Am. Meteorol. Soc.* **2017**, *98*, 2397–2409. [[CrossRef](#)]
36. Balconi, M.; Brusoni, S.; Orsenigo, L. In Defence of the Linear Model: An Essay. *Res. Policy* **2010**, *39*, 1–13. [[CrossRef](#)]
37. Babar, I.; Ayed, H.; Chand, S.; Suhail, M.; Khan, Y.A.; Marzouki, R. Modified Liu Estimators in the Linear Regression Model: An Application to Tobacco Data. *PLoS ONE* **2021**, *16*, e0259991. [[CrossRef](#)] [[PubMed](#)]

38. Mašek, J.; Tumajer, J.; Lange, J.; Vejpusťková, M.; Kašpar, J.; Šamonil, P.; Chuman, T.; Kolář, T.; Rybníček, M.; Jeníček, M.; et al. Shifting Climatic Responses of Tree Rings and NDVI along Environmental Gradients. *Sci. Total Environ.* **2024**, *908*, 168275. [[CrossRef](#)] [[PubMed](#)]
39. Prasai, R. Using Google Earth Engine for the Complete Pipeline of Temporal Analysis of NDVI in Chitwan National of Nepal. *Res. Sq.* **2022**, *3*, 151–157. [[CrossRef](#)]
40. Huang, E.; Chen, Y.; Fang, M.; Zheng, Y.; Yu, S. Environmental Drivers of Plant Distributions at Global and Regional Scales. *Glob. Ecol. Biogeogr.* **2021**, *30*, 697–709. [[CrossRef](#)]
41. Johnson, D.M.; Rosales, A.; Mueller, R.; Reynolds, C.; Frantz, R.; Anyamba, A.; Pak, E.; Tucker, C. Usa Crop Yield Estimation with Modis Ndvi: Are Remotely Sensed Models Better than Simple Trend Analyses? *Remote Sens.* **2021**, *13*, 4227. [[CrossRef](#)]
42. Karkauskaite, P.; Tagesson, T.; Fensholt, R. Evaluation of the Plant Phenology Index (PPI), NDVI and EVI for Start-of-Season Trend Analysis of the Northern Hemisphere Boreal Zone. *Remote Sens.* **2017**, *9*, 485. [[CrossRef](#)]
43. le Maire, G.; Marsden, C.; Nouvellon, Y.; Grinand, C.; Hakamada, R.; Stape, J.L.; Laclau, J.P. MODIS NDVI Time-Series Allow the Monitoring of Eucalyptus Plantation Biomass. *Remote Sens. Environ.* **2011**, *115*, 2613–2625. [[CrossRef](#)]
44. Barichivich, J.; Briffa, K.R.; Myneni, R.; van der Schrier, G.; Dorigo, W.; Tucker, C.J.; Osborn, T.J.; Melvin, T.M. Temperature and Snow-Mediated Moisture Controls of Summer Photosynthetic Activity in Northern Terrestrial Ecosystems between 1982 and 2011. *Remote Sens.* **2014**, *6*, 1390–1431. [[CrossRef](#)]
45. Camberlin, P.; Martiny, N.; Philippon, N.; Richard, Y. Determinants of the Interannual Relationships between Remote Sensed Photosynthetic Activity and Rainfall in Tropical Africa. *Remote Sens. Environ.* **2007**, *106*, 199–216. [[CrossRef](#)]
46. Roznik, M.; Boyd, M.; Porth, L. Improving Crop Yield Estimation by Applying Higher Resolution Satellite NDVI Imagery and High-Resolution Cropland Masks. *Remote Sens. Appl. Soc. Environ.* **2022**, *25*, 100693. [[CrossRef](#)]
47. Mbatha, N.; Xulu, S. Time Series Analysis of MODIS-Derived NDVI for the Hluhluwe-Imfolozi Park, South Africa: Impact of Recent Intense Drought. *Climate* **2018**, *6*, 95. [[CrossRef](#)]
48. Kinyanjui, M.J. NDVI-Based Vegetation Monitoring in Mau Forest Complex, Kenya. *Afr. J. Ecol.* **2010**, *49*, 165–174. [[CrossRef](#)]
49. Gkatzoura, P.E.; Perakis, K. Analysis of Urban Heat Island (UHI) through Climate Engine and Arcgis Pro in Different Cities of Bulgaria. In Proceedings of the Eighteenth International Scientific Conference, Sofia, Bulgaria, 19–21 October 2022.
50. Guan, L.; Yang, J.; Bell, J.M. Cross-Correlations between Weather Variables in Australia. *Build. Environ.* **2007**, *42*, 1054–1070. [[CrossRef](#)]
51. Schmidt, A.F.; Finan, C. Linear Regression and the Normality Assumption. *J. Clin. Epidemiol.* **2018**, *98*, 146–151. [[CrossRef](#)] [[PubMed](#)]
52. Zhao, M.; Peng, C.; Xiang, W.; Deng, X.; Tian, D.; Zhou, X.; Yu, G.; He, H.; Zhao, Z. Plant Phenological Modeling and Its Application in Global Climate Change Research: Overview and Future Challenges. *Environ. Rev.* **2013**, *21*, 1–14. [[CrossRef](#)]
53. Wu, S.; Di, B.; Ustin, S.L.; Wong, M.S.; Adhikari, B.R.; Zhang, R.; Luo, M. Dynamic Characteristics of Vegetation Change Based on Reconstructed Heterogenous NDVI in Seismic Regions. *Remote Sens.* **2023**, *15*, 299. [[CrossRef](#)]
54. Aktas, A.F.; Berk Ustundag, B. Phenology Based NDVI Time-Series Compensation for Yield Estimation Analysis. In Proceedings of the 2017 6th International Conference on Agro-Geoinformatics, Agro-Geoinformatics, Fairfax, VA, USA, 7–10 August 2017; Institute of Electrical and Electronics Engineers Inc.: Piscataway, NJ, USA, 2017.
55. Rodrigo, O.B. Innovación y Tecnología Para Mejorar La Sustentabilidad Agrícola En El Sector Pecuário. *Rev. Colomb. Cienc. Pecu.* **2019**, *32*, 22–33.
56. Huang, J.; Wang, X.; Li, X.; Tian, H.; Pan, Z. Remotely Sensed Rice Yield Prediction Using Multi-Temporal NDVI Data Derived from NOAA's-AVHRR. *PLoS ONE* **2013**, *8*, e70816. [[CrossRef](#)] [[PubMed](#)]
57. Ferrer, M.; Echeverría, G.; Pereyra, G.; Gonzalez-Neves, G.; Pan, D.; Mirás-Avalos, J.M. Mapping Vineyard Vigor Using Airborne Remote Sensing: Relations with Yield, Berry Composition and Sanitary Status under Humid Climate Conditions. *Precis. Agric.* **2020**, *21*, 178–197. [[CrossRef](#)]
58. Tenreiro, T.R.; García-Vila, M.; Gómez, J.A.; Jiménez-Berni, J.A.; Fereres, E. Using NDVI for the Assessment of Canopy Cover in Agricultural Crops within Modelling Research. *Comput. Electron. Agric.* **2021**, *182*, 106038. [[CrossRef](#)]
59. Chiang, S.H.; Ulloa, N.I. Mapping and Tracking Forest Burnt Areas in the Indio Maiz Biological Reserve Using Sentinel-3 SLSTR and VIIRS-DNB Imagery. *Sensors* **2019**, *19*, 5423. [[CrossRef](#)] [[PubMed](#)]
60. Chemura, A.; Mutanga, O.; Dube, T. Integrating Age in the Detection and Mapping of Incongruous Patches in Coffee (*Coffea arabica*) Plantations Using Multi-Temporal Landsat 8 NDVI Anomalies. *Int. J. Appl. Earth Obs. Geoinf.* **2017**, *57*, 1–13. [[CrossRef](#)]
61. Chen, D.; Zhao, Q.; Jiang, P.; Li, M. Incorporating Ecosystem Services to Assess Progress towards Sustainable Development Goals: A Case Study of the Yangtze River Economic Belt, China. *Sci. Total Environ.* **2022**, *806*, 151277. [[CrossRef](#)] [[PubMed](#)]
62. Guerron Barahona, A.M.; Viera Arroyo, W.F.; Campaña Cruz, D.F.; Vasquez Rojas, L.; Montufar Salcedo, C.L. Aplicación de Índices Vegetales (Banda Roja e Infrarrojo Cercano) En Plantaciones de Aguacate. *Siembra* **2022**, *9*, e3371. [[CrossRef](#)]
63. Rahman, M.S.; Di, L.; Shrestha, R.; Yu, E.G.; Lin, L.; Kang, L.; Deng, M. Comparison of Selected Noise Reduction Techniques for MODIS Daily NDVI: An Empirical Analysis on Corn and Soybean. In Proceedings of the 2016 Fifth International Conference on Agro-Geoinformatics (Agro-Geoinformatics), Tianjin, China, 18–20 July 2016.
64. Guan, S.; Fukami, K.; Matsunaka, H.; Okami, M.; Tanaka, R.; Nakano, H.; Sakai, T.; Nakano, K.; Ohdan, H.; Takahashi, K. Assessing Correlation of High-Resolution NDVI with Fertilizer Application Level and Yield of Rice and Wheat Crops Using Small UAVs. *Remote Sens.* **2019**, *11*, 112. [[CrossRef](#)]

65. Belmahi, M.; Hanchane, M.; Krakauer, N.Y.; Kessabi, R.; Bouayad, H.; Mahjoub, A.; Zouhri, D. Analysis of Relationship between Grain Yield and NDVI from MODIS in the Fez-Meknes Region, Morocco. *Remote Sens.* **2023**, *15*, 2707. [[CrossRef](#)]
66. Rivera, L.B.; Bonilla, B.M.; Obando-Vidal, F. Processing Multispectral Imaging Captured by Drones to Evaluate the Normalized Difference Vegetation Index of Castillo Coffee Plantations. *Cienc. Tecnol. Agropecu.* **2021**, *22*, 1578. [[CrossRef](#)]
67. Campos, B.F.D.; Alves, H.M.R.; Volpato, M.M.L.; Inácio, F.D.; Silva, V.A. Distribuição do Ndvi e Exposição de Vertentes em Áreas Cafeeiras em Santo Antônio do Amparo, MG 1. In Proceedings of the X Simpósio de Pesquisa dos Cafés do Brasil, Vitoria, Brazil, 8–11 October 2019.
68. André, M.B.P.; De, M.A.C.; Rocha, J.; Chaves, M. Modelagem Espectro-Temporal Do NDVI Obtido de Imagens Landsat 7 e 8 Aplicado Na Cafeicultura. *XiX Simpósio Bras. De Sensoriamento Remoto* **2019**, *19*, 96622.
69. Dos Santos, L.M.; E S Ferraz, G.A.; Marin, D.B.; Carvalho, M.A.; Guimarães, R.J.; O Alecrim, A.D. *Ndvi Aplicado em Imagens Multiespectrais de Cafeeiros Sadios e Cafeeiros Infestados Com Bicho-Mineiro Ndvi Applied in Multispectral Images of Healthy Coffee and Coffee Infested with “Bicho-Mineiro”*. 2020. XLIX Congresso Brasileiro de Engenharia Agrícola—Brasil. Available online: <https://ainfo.cnptia.embrapa.br/digital/bitstream/doc/1143370/1/NDVI-APLICADO-EM-IMAGENS-2020-1.pdf> (accessed on 25 July 2024).
70. Chuai, X.W.; Huang, X.J.; Wang, W.J.; Bao, G. NDVI, Temperature and Precipitation Changes and Their Relationships with Different Vegetation Types during 1998–2007 in Inner Mongolia, China. *Int. J. Climatol.* **2013**, *33*, 1696–1706. [[CrossRef](#)]
71. Jiao, K.; Gao, J.; Liu, Z. Precipitation Drives the Ndvi Distribution on the Tibetan Plateau While High Warming Rates May Intensify Its Ecological Droughts. *Remote Sens.* **2021**, *13*, 1305. [[CrossRef](#)]
72. Zhang, H.; Liu, L.; Jiao, W.; Li, K.; Wang, L.; Liu, Q. Watershed Runoff Modeling through a Multi-Time Scale Approach by Multivariate Empirical Mode Decomposition (MEMD). *Environ. Sci. Pollut. Res.* **2022**, *29*, 2819–2829. [[CrossRef](#)] [[PubMed](#)]
73. Turvey, C.G.; McLaurin, M.K. Applicability of the Normalized Difference Vegetation Index (NDVI) in Index-Based Crop Insurance Design. *Weather Clim. Soc.* **2012**, *4*, 271–284. [[CrossRef](#)]
74. Skok, G. Precipitation Attribution Distance. *Atmos. Res.* **2023**, *295*, 106998. [[CrossRef](#)]
75. Gomez, C.; Despinoy, M.; Hamon, S.; Salmon, P.; Salmon, D.; Akaffou, D.S.; Legnate, H.; de Kochko, A.; Mangeas, M.; Poncet, V. Shift in Precipitation Regime Promotes Interspecific Hybridization of Introduced *Coffea* Species. *Ecol. Evol.* **2016**, *6*, 3240–3255. [[CrossRef](#)] [[PubMed](#)]
76. Parada Molina, P.C.; Cervantes Pérez, J.; Ruiz Molina, V.E.; Cerdán Cabrera, C.R. Efectos de La Variabilidad de La Precipitación En La Fenología Del Café: Caso Zona Cafetalera Xalapa-Coatepec, Veracruz, Mex. *Ing. Región* **2020**, *24*, 61–71. [[CrossRef](#)]
77. Drinnan, J.E.; Menzel, C.M. Temperature Affects Vegetative Growth and Flowering of Coffee (*Coffea arabica* L.). *J. Hortic. Sci.* **1995**, *70*, 25–34. [[CrossRef](#)]
78. Davis, A.P.; Gargiulo, R.; Almeida, I.N.d.M.; Caravela, M.I.; Denison, C.; Moat, J. Hot Coffee: The Identity, Climate Profiles, Agronomy, and Beverage Characteristics of *Coffea Racemosa* and *C. Zanguebariae*. *Front. Sustain. Food Syst.* **2021**, *5*, 740137. [[CrossRef](#)]
79. Gerson, A.A. *Comportamiento de Tres Variedades de Café (Coffea arabica L.) en El Valle del Perené, Junín-Perú*; Universidad Nacional Agraria La Molina: Lima, Peru, 2016.
80. Martinez, A.d.I.I.; Labib, S.M. Demystifying Normalized Difference Vegetation Index (NDVI) for Greenness Exposure Assessments and Policy Interventions in Urban Greening. *Environ. Res.* **2023**, *220*, 115155. [[CrossRef](#)] [[PubMed](#)]
81. Johnson, M.D.; Hsieh, W.W.; Cannon, A.J.; Davidson, A.; Bédard, F. Crop Yield Forecasting on the Canadian Prairies by Remotely Sensed Vegetation Indices and Machine Learning Methods. *Agric. For. Meteorol.* **2016**, *218–219*, 74–84. [[CrossRef](#)]
82. Garcia-Garcia, D.; Reynafarje la Rosa, X.; Grados Bedoya, D.; Schrevels, E. Linear Mixed Model Analysis of NDVI-Based Canopy Coverage, Extracted from Sequential UAV Multispectral Imagery of an Open Field Tomato Irrigation Experiment. *Comput. Electron. Agric.* **2021**, *189*, 106399. [[CrossRef](#)]
83. Bolton, D.K.; Friedl, M.A. Forecasting Crop Yield Using Remotely Sensed Vegetation Indices and Crop Phenology Metrics. *Agric. For. Meteorol.* **2013**, *173*, 74–84. [[CrossRef](#)]
84. Xu, C.; Katchova, A.L. Predicting Soybean Yield with NDVI Using a Flexible Fourier Transform Model. *J. Agric. Appl. Econ.* **2019**, *51*, 402–416. [[CrossRef](#)]

Disclaimer/Publisher’s Note: The statements, opinions and data contained in all publications are solely those of the individual author(s) and contributor(s) and not of MDPI and/or the editor(s). MDPI and/or the editor(s) disclaim responsibility for any injury to people or property resulting from any ideas, methods, instructions or products referred to in the content.